Dyes and Pigments 113 (2015) 189–199

Contents lists available at ScienceDirect

Dyes and Pigments

journal homepage: www.elsevier.com/locate/dyepig

Chemiluminescence properties of luminol related *o*-hydroxybenzimidazole analogues: Experimental and DFT based approach to photophysical properties

Mininath S. Deshmukh, Nagaiyan Sekar*

Tinctorial Chemistry Group, Dyestuff Technology Department, Institute of Chemical Technology (Formerly UDCT), N.P. Marg, Matunga, Mumbai 400019, Maharashtra, India

ARTICLE INFO

Article history:
Received 5 May 2014
Received in revised form
1 August 2014
Accepted 10 August 2014
Available online 20 August 2014

Keywords:
Luminol–isoluminol
Chemiluminescence
Fluorescence
Solvatochromism
ESIPT
TD-DFT

ABSTRACT

Novel luminol–isoluminol derivatives containing o-hydroxyphenyl benzimidazole unit were synthesized from aromatic aldehydes and diaminophthalates followed by heating under reflux with hydrazine hydrate. The chemiluminescent properties were studied in hydrogen peroxide, potassium hexacyanoferrate(III) and sodium hydroxide solution. The chemiluminescence properties were compared with the standard luminol and isoluminol systems it was observed that the chemiluminescence properties of the novel derivatives were superior to luminol and isoluminol. Density Functional Theory computations have been used in order to have a greater understanding of the structural, molecular, electronic and photophysical properties. The experimental absorption and emission wavelength values were in good agreement with the computed vertical excitation and emission values.

1. Introduction

Compounds exhibiting chemiluminescence (CL) are extensively used for various biomicroanalyses due to their high selectivity and sensitivity [1]. In recent years, chemiluminescence has been an attractive detection technique in the high-performance liquid chromatography (HPLC) [2]. A convenient labelling reagent having a luminol moiety has not been reported due to the fact that the CL intensity is always low and the synthesis method is difficult. On the other hand, various reagents containing an isoluminol moiety like isoluminolisothiocyanate (ILITC) [3], *N*-aminobutyl-*N*-ethyl-isoluminol (ABEI) [4,5], 4,5-diaminophthalhydrazide (DPH) [6] and 6-aminomethylphthalhydrazide (6-AMP) [7] have been widely used for the microanalyses of biological compounds. The introduction of electron donating groups (alkyl or aryl) on the amino group of luminol causes a decrease in the CL intensity. On the other hand, the electron donating group (alkyl or aryl) on the amino of isoluminol causes an increase in the CL intensity [8,9].

In recent years, there has been an increasing interest in molecules with excited state intramolecular proton transfer (ESIPT) because of their wide applications in molecular probes [10], luminescent materials [11,12], metal ion sensors [13–15], organic light emitting devices (OLEDs) [16] and molecular logic gates [17]. In the case of barrierless excited state intramolecular proton transfer (ESIPT), a covalently attached proton, typically of a hydroxyl or amino group, in the electronically excited state migrates to a neighbouring hydrogen-bonded atom less than 2 Å away [18]. A large Stokes shift is a desired characteristic for fluorophores because self-absorption or the inner filter effect can be avoided and the fluorescence analysis can be enhanced [19]. It is difficult to increase the Stokes shift of the conventional fluorophores by chemical modification.

During photoexcitation to the first excited state, the acidity of the acidic center (proton) and the basicity of the basic center (imidazole nitrogen) increase because of a change in the charge density of the chromophore. This leads to the migration of the proton from the acidic centre to the basic center via the hydrogen bond coordinate to give the phototautomer. The phototautomer formed in the excited state emits light and thermally equilibrates back to the ground state with the proton bound to its original atom. Generally these processes are extremely fast and several studies have shown subpicosecond reaction rates for a variety of molecules [20,21]. In this process a significant amount of excited-state energy is dissipated, the phototautomer fluoresces at a lower

* Corresponding author. Tel.: +91 22 3361 1111/2707; fax: +91 22 3361 1020.
E-mail addresses: n.sekar@ictmumbai.edu.in, nethi.sekar@gmail.com (N. Sekar).

http://dx.doi.org/10.1016/j.dyepig.2014.08.009
0143-7208/

energy with an unusually larger Stokes shift (up to 10,000 cm^{-1}) [22].

Therefore, considering the wide applications and importance of ESIPT inspired molecules and in continuation of our research work on fluorescent materials [23–25] herein, we report the synthesis of novel chemiluminescent ESIPT inspired substituted **HPBI** (hydroxyphenyl benzimidazole) fluorophores and their photophysical properties are correlated with the computational results obtained from DFT [B3LYP/6-31G(d)] and reported analogues.

2. Experimental section

2.1. Materials and methods

All the commercial reagents and solvents were used as received or purified using standard procedures. The reaction was monitored by TLC using 0.25 mm silica gel 60 F_{254} precoated plates, which were visualized with UV light. Melting points were measured on standard melting point apparatus from Sunder Industrial Product, Mumbai, and are uncorrected. The FT-IR spectra were recorded on Jasco 4100 using ATR accessory. ^{1}H NMR spectra were recorded on VARIAN Inc. (USA) 400/600-MHz instrument using TMS as an internal standard and DMSO-d_6 as the solvent at room temperature. Mass spectra were recorded on Finnigan mass spectrometer. Simultaneous DSC-TGA measurements were performed out on SDT Q 600 v8.2 Build 100 model of TA instruments Waters (India) Pvt. Ltd. The UV–visible absorption and emission spectra were performed on a Perkin–Elmer Lamda 25 and Varian Cary Eclipse at room temperature. Quantum yields were obtained by using quinine sulfate (0.54 in ethanol) as reference [26]. NaOH solution of the hydrogen peroxide and potassium hexacyanoferrate(III) as a oxidizing agent for chemiluminescence measurements.

2.2. Computational methods

The quantum chemical calculations were performed using Gaussian 09 [27] software at the B3LYP/6-31G(d) level of theory. The ground state (S_0) geometry of the synthesized compounds has been obtained by full optimization of the structural parameters using DFT employing 6-31G(d) basis set [28]. The B3LYP method combines Becke's three parameter exchange functional (B3) [29] with the nonlocal correlation functional by Lee, Yang, and Parr (LYP) [30]. The vibrational frequencies at the optimized structures were computed using the same method to verify that the optimized structures correspond to local minima on the energy surface [31]. The vertical excitation energy and oscillator strengths at ground state equilibrium geometries were calculated using TD-DFT at the same level of theory [32–34]. The low-lying first singlet excited states (S_1) of the compounds were relaxed using TD-DFT to obtain the minimum energy geometry. The difference between the energies of the optimized geometries at the first singlet excited state and the ground state was used in computing the emissions [35,36]. Frequency computations were also carried out on the optimized geometry of the low-lying vibronically relaxed first excited state of conformers to ascertain the validity of structure and no imaginary frequencies were found. All the computations in solvents of different polarities were carried out using the Polarizable Continuum Model (PCM) [37].

2.3. Examination of the chemiluminescent properties

2.3.1. Standard procedure

The chemiluminescence reaction was initiated by the simultaneous automatic injections of 100 μL of hydrogen peroxide solution and 100 mL of potassium hexacyanoferrate(III) solution dissolved in sodium hydroxide to the 100 μL portion of a 10 nM solution of each chemiluminophore. The chemiluminescence intensities were recorded immediately after the injection of oxidizing agent solution. The integrated photon counts for 1 min after the injections were explained as the chemiluminescence intensities.

2.3.2. Optimization of the chemiluminescence conditions

To establish the optimum chemiluminescence conditions the concentrations of the oxidizing reagents (hydrogen peroxide, potassium hexacyanoferrate(III) and sodium hydroxide) were varied one at a time. The temporarily settled conditions were DMF solution of chemiluminophore, 5.0 mM hydrogen peroxide and 5.0 mM potassium hexacyanoferrate(III) prepared in 1.5 M sodium hydroxide.

2.3.3. Fluorescence of the CL reaction product

To 200 μL of the 1 mM stock solution of chemiluminophores, 50 μL of 10 mM potassium hexacyanoferrate(III) in 1.5 M NaOH and 50 μL of 10 mM hydrogen peroxide were added and allowed to stand for 1 h at room temperature. The fluorescence emission maxima, excitation and relative intensities of the resulting mixtures were recorded in the fluorescence spectrometer.

2.4. Synthesis and characterization

The synthetic schemes for the preparation of the *o*-hydroxybenzimidazole derivatives are shown in Scheme 1. Dimethyl 4,5-diaminophthalate (**6**) and dimethyl 4,3-diaminophthalate (**6'**) were prepared by the reported procedure [38] from 4-nitrophthalic acid **(1)**.

2.4.1. General procedure for the preparation of benzimidazole

To a solution of diaminodimethylphthalate **(6** or **6')** (0.5g, 2.2 mmol), and *o*-hydroxybenzaldehyde (**a** or **b** or **c)** (2.2 mmol) in ethanol (5 mL), Phosphorus trichloride (0.22 mL, 2.6 mmol) was added drop wise over a period of 15 min.The temperature was maintained at 40–45 °C during complete addition. The mixture was heated under reflux for 6 h. Solid product separated on pouring reaction mass to crushed ice to afford dimethylphthalate HPBI (**7a**–**7b** and **7'a**–**7'c)**. The product was recrystallized from ethanol.

*2.4.1.1. Dimethyl 2-(4-(diethylamino)-2-hydroxyphenyl)-1H-benzo[d]imidazole-5,6-dicarboxylate **(7a)**.* Yield: 77%; Melting point: 212–214 °C; FT-IR: 3326 (–OH), 2953 (–NH), 1720 (–C=O), 1608, 1556 (C=C, C=N ring stretching), 1271, 1195 (C–O stretching) cm^{-1}. ^{1}H NMR (DMSO-d_6): δ 13.09 (s, 1H, –OH), 12.36 (s, 1H, –NH), 7.86 (s, 2H, Ar–H), 7.81 (d, 1H, Ar–H, J = 9.0 Hz), 6.40 (d, 1H, Ar–H, J = 7.5 Hz), 6.20 (s, 1H, Ar–H), 3.81 (s, 6H, $-OCH_3$), 3.40 (q, 4H, $-NCH_2$), 1.13 (t, 6H, $-CH_3$); ^{1}H NMR (D_2O exchange): δ 7.82 (s, 2H, Ar–H), 7.74 (d, 1H, Ar–H, J = 9.0 Hz), 6.35 (d, 1H, Ar–H, J = 8.0 Hz), 6.15 (s, 1H, Ar–H), 3.78 (s, 6H, $-OCH_3$), 3.33 (q, 4H, $-NCH_2$), 1.08 (t, 6H, $-CH_3$); ^{13}C NMR (DMSO-d_6, 125.8 MHz): δ 168.29, 168.18, 160.24, 156.68, 151.26, 145.24, 144.97, 128.43, 118.34, 117.23, 112.56, 104.36, 100.06, 97.93(s), 52.43(s), 44.14(s), 12.88(s); HRMS: Calcd for $C_{21}H_{24}N_3O_5$ $[M+H]^+$ 398.1716, found 398.2210; Mass m/z: 398.20 $[M+H]^+$.

*2.4.1.2. Dimethyl 2-(2-hydroxyphenyl)-1H-benzo[d]imidazole-5,6-dicarboxylate **(7b)**.* Yield: 72%; Melting point: 240–242 °C; FT-IR: 3321(–OH), 2945(–NH), 1738, 1686 (–C=O), 1639, 1611, 1557 (C=C, C=N ring stretching), 1242, 1213 (C–O stretching) cm^{-1}; ^{1}H NMR (DMSO-d_6): (–OH and –NH proton exchange with solvent) δ 8.24 (d, 1H, Ar–H, J = 8.0 Hz), 8.07 (s, 2H, Ar–H), 7.51 (t, 1H, Ar–H, J = 8.0 Hz), 7.19 (d, 1H, Ar–H, J = 8.0 Hz), 7.08 (t, 1H, Ar–H, J = 8.0 Hz), 3.85 (s, 6H, $-OCH_3$); ^{1}H NMR (D_2O exchange):

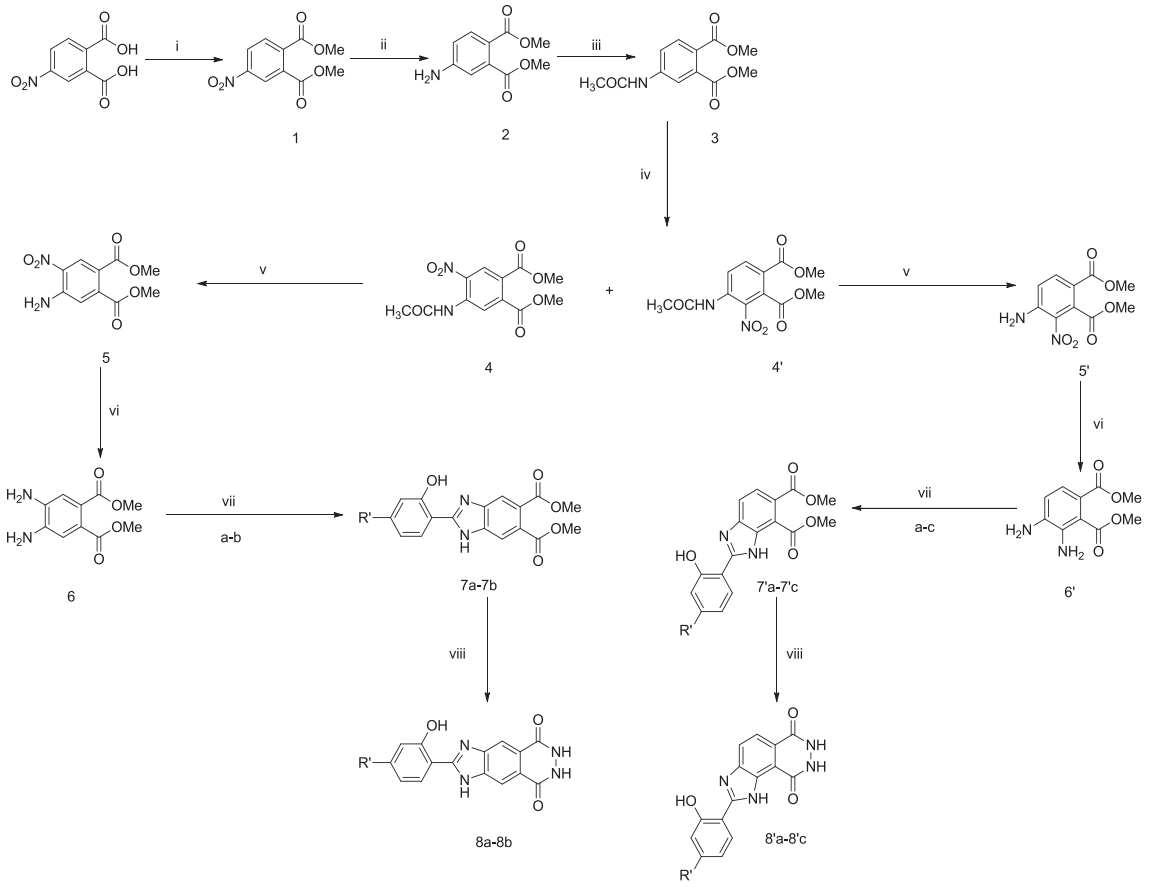

Reagents and conditions: **(i)** *H_2SO_4/ methanol, reflux,10 h.* **(ii)** *H_2/Pd-C, methanol, rt.* **(iii)** *toluene, acetic anhydride, 80 °C, 4 h.* **(iv)** *90% fuming HNO_3, 0-5 °C.* **(v)** *conc. H_2SO_4, 30 min, rt.* **(vi)** *H_2/Pd-C, methanol, rt.* **(vii)** *PCl_3, ethanol, reflux, 4 h.* **(viii)** *methanol, hydrazine hydrate, triethylamine, reflux 4 h.*

Scheme 1. Synthesis of dimethyl phthalate and phthalazine substituted **HPBI** derivatives (**7a**–**7b, 7'a**–**7'c, 8a**–**8b** and **8'a**–**8'c**).

δ 8.03 (s, 2H, Ar–H), 8.01 (d, 1H, Ar–H, J = 8.0 Hz), 7.49 (t, 1H, Ar–H, J = 8.0 Hz), 7.10 (d, 1H, Ar–H, J = 8.5 Hz), 7.06 (t, 1H, Ar–H, J = 8.0 Hz), 3.81 (s, 6H, $-OCH_3$); ^{13}C NMR (DMSO-d_6, 125.8 MHz): δ 167.03(s), 157.81, 151.45, 134.73, 134.37, 129.04, 127.88, 119.80(s), 117.32(s), 115.29(s), 109.77, 52.79(s); HRMS: Calcd for $C_{17}H_{15}N_2O_5$, $[M+H]^+$ 327.0981, found 327.1432; Mass m/z: 327.10 $[M+H]^+$.

*2.4.1.3. Dimethyl 2-(4-(diethylamino)-2-hydroxyphenyl)-1H-benzo [d]imidazole-4,5-dicarboxylate **(7'a)**.* Yield: 76%; Melting point: 208–210 °C; FT-IR: 3365 (–OH), 2797 (–NH), 1731 (–C=O), 1608, 1558 (C=C, C=N ring stretching), 1316, 1246 (C–O stretching) cm^{-1}; ^{1}H NMR (DMSO-d_6): δ 13.17 (s, 1H, –OH), 12.41 (s, 1H, –NH), 7.79 (d, 1H, Ar–H, J = 9.0 Hz), 7.75 (d, 1H, Ar–H, J = 7.5 Hz), 7.64 (d, 1H, Ar–H, J = 8.0 Hz), 6.39 (d, 1H, Ar–H, J = 9.0 Hz), 6.17 (s, 1H, Ar–H), 3.89 (s, 3H, $-OCH_3$), 3.83 (s, 3H, $-OCH_3$), 3.38 (q, 4H, $-NCH_2$), 1.13 (t, 6H, $-CH_3$); ^{1}H NMR (D_2O exchange): δ 7.74 (d, 1H, Ar–H, J = 6.0 Hz), 7.70 (d, 1H, Ar–H, J = 6.0 Hz), 7.64 (d, 1H, Ar–H, J = 7.5 Hz), 6.34 (d, 1H, Ar–H, J = 9.0 Hz), 6.13 (s, 1H, Ar–H), 3.86 (s, 3H, $-OCH_3$), 3.78 (s, 3H, $-OCH_3$), 3.32 (q, 4H, $-NCH_2$), 1.07 (t, 6H, $-CH_3$); ^{13}C NMR (DMSO-d_6, 125.8 MHz): δ 167.55, 167.57, 160.41, 156.00, 150.65, 139.29, 137.19, 128.29, 123.61, 121.61, 112.13, 104.29, 99.84, 97.91(s), 52.73(s), 44.12(s), 12.89(s); HRMS: Calcd for $C_{21}H_{24}N_3O_5$, $[M+H]^+$ 398.1716, found 398.2211; Mass m/z: 398.20 $[M+H]^+$.

*2.4.1.4. Dimethyl 2-(2-hydroxyphenyl)-1H-benzo[d]imidazole-4,5-dicarboxylate **(7'b)**.* Yield: 70%; Melting point: 192–194 °C; FT-IR: 3316 (–OH), 2967 (–NH), 1711 (–C=O), 1633, 1558 (C=C, C=N ring stretching), 1306, 1264 (C–O stretching) cm^{-1}; ^{1}H NMR (DMSO-d_6): (–OH and –NH proton exchange with solvent) δ 8.17 (d, 1H, Ar–H, J = 7.5 Hz), 7.86 (dd, 2H, Ar–H, J = 8.5 Hz), 7.47 (t, 1H, Ar–H, J = 8.5 Hz), 7.10 (d, 1H, Ar–H, J = 7.5 Hz), 7.06 (t, 1H, Ar–H, J = 8.0 Hz), 3.93 (s, 3H, $-OCH_3$), 3.85 (s, 3H, $-OCH_3$); ^{1}H NMR (D_2O exchange): δ 8.00 (d, 1H, Ar–H, J = 8.0 Hz), 7.81 (dd, 2H, Ar–H, J = 8.5 Hz), 7.44 (t, 1H, Ar–H, J = 8.5 Hz), 7.06 (t, 1H, Ar–H, J = 6.0 Hz), 7.04 (d, 1H, Ar–H, J = 8.5 Hz), 3.89 (s, 3H, $-OCH_3$), 3.80 (s, 3H, $-OCH_3$); ^{13}C NMR (DMSO-d_6, 125.8 MHz): δ 166.53(s), 158.21, 153.16, 136.81, 134.21, 129.09, 125.30, 124.22, 119.88(s), 117.60(s), 115.62, 111.13, 53.24(s); HRMS: Calcd for $C_{17}H_{15}N_2O_5$, $[M+H]^+$ 327.0981, found 327.1435; Mass m/z: 327.10 $[M+H]^+$.

*2.4.1.5. Dimethyl 2-(2,4-dihydroxyphenyl)-1H-benzo[d]imidazole-4,5-dicarboxylate **(7'c)**.* Yield: 80%; Melting point: 242–244 °C; FT-IR: 3387, 3286 (−OH), 2955 (−NH), 1731, 1695 (−C═O), 1633, 1558 (C═C, C═N ring stretching), 1306, 1264 (C–O stretching) cm^{-1}; ^1H NMR (DMSO-d_6): (Two −OH proton is exchange in solvent) δ 10.69 (br s, 1H, −NH), 8.06 (d, 1H, Ar–H, J = 8.5 Hz), 7.89 (d, 1H, Ar–H, J = 8.5 Hz), 7.81 (d, 1H, Ar–H, J = 8.5 Hz), 6.61 (s, 1H, Ar–H), 6.53 (dd, 1H, Ar–H, J = 2.5 Hz and 6.5 Hz), 3.94 (s, 3H, $-OCH_3$), 3.81 (s, 3H, $-OCH_3$); ^1H NMR (D_2O exchange): δ 7.85 (d, 1H, Ar–H, J = 8.5 Hz), 7.82 (d, 1H, Ar–H, J = 8.5 Hz), 7.76 (d, 1H, Ar–H, J = 8.5 Hz), 6.51 (dd, 1H, Ar–H, J = 2.5 Hz and 6.0 Hz), 6.47 (d, 1H, Ar–H, J = 2.5 Hz), 3.89 (s, 3H, $-OCH_3$), 3.79 (s, 3H, $-OCH_3$); ^{13}C NMR (DMSO-d_6, 125.8 MHz): δ 166.64, 165.57, 164.31, 160.45, 152.15, 135.33, 131.41, 125.47, 119.50, 115.98, 109.27, 103.34(s), 101.04(s), 53.43, 53.18; HRMS: Calcd for $C_{17}H_{15}N_2O_6$, $[M+H]^+$ 343.0930, found 343.1392; Mass m/z: 343.67 $[M+H]^+$.

2.4.2. General procedure for the preparation of phthalazine

The solution of dimethylphthalate HPBI (**7a,7b** and **7'a–7'c)** (1 mmol) and hydrazine hydrate (1.5 mL) in methanol (5 mL) was heated under reflux in presence of triethylamine (1.5 mL) for 2 h. The product precipitated during the reaction. The crude product was recrystallized from *N,N'*-dimethylacetamide to give the compounds **8a,8b** and **8'a–8'c** respectively. The low solubility of this compounds made the ^{13}C NMR characterization of these substrates not possible. Only the IR, ^1H NMR, mass and HRMS are reported.

*2.4.2.1. 2-(4-(Diethylamino)-2-hydroxyphenyl)-6,7-dihydro-1H-imidazo[4,5-g]phthalazine-5,8-dione **(8a)**.* Yield: 88%; Melting point: 186–188 °C; FT-IR: 3233 (−OH), 2960, 2869 (−NH), 1644 (−C═O amide), 1609, 1531 (C═C, C═N ring stretching), 1315, 1252 (C–O stretching) cm^{-1}; ^1H NMR (DMSO-d_6): δ 13.17 (br s, 1H, −OH), 12.53 (br s, 1H, −NH), 11.30 (br s, 2H, −NH), 8.11 (br s, 2H, Ar–H), 7.85 (d, 1H, Ar–H, J = 9.0 Hz), 6.43 (dd, 1H, Ar–H, J = 2.0 Hz and J = 7.0 Hz), 6.21 (d, 1H, Ar–H, J = 2.5 Hz), 3.41 (q, 4H, $-NCH_2$), 1.14 (t, 6H, −CH3); ^1H NMR (D_2O exchange): δ 8.14 (br s, 2H, Ar–H), 7.81 (d, 1H, Ar–H, J = 9.0 Hz), 6.37 (dd, 1H, Ar–H, J = 2.0 Hz and J = 7.0 Hz), 6.18 (d, 1H, Ar–H, J = 2.0 Hz), 3.37 (q, 4H, $-NCH_2$), 1.11 (t, 6H, −CH3); HRMS: Calcd for $C_{19}H_{20}N_5O_3$, $[M+H]^+$ 366.1566, found 366.2037; Mass m/z: 366.22 $[M+H]^+$.

*2.4.2.2. 2-(2-hydroxyphenyl)-6,7-dihydro-1H-imidazo[4,5-g]phthalazine-5,8-dione **(8b)**.* Yield: 78%; Melting point: 250–252 °C; FT-IR: 3213 (−OH), 2965, 2866 (−NH), 1636 (−C═O amide), 1620, 1540 (C═C, C═N ring stretching), 1350, 1268 (C–O stretching) cm^{-1}; ^1H NMR (DMSO-d_6): δ 13.56 (s, 1H, ═OH), 12.52 (s, 1H, ═NH), 11.38 (br s, 2H, ═NH), 8.29 (s, 2H, Ar–H), 8.16 (dd, 1H, Ar–H, J = 1.5 Hz and J = 6.5 Hz), 7.46 (t, 1H, Ar–H, J = 8.5 Hz), 7.08 (m, 2H, Ar–H); ^1H NMR (D_2O exchange): δ 8.30 (s, 1H, Ar–H), 8.12 (s, 1H, Ar–H), 8.09 (dd, 1H, Ar–H, J = 1.5 Hz and J = 6.5 Hz), 7.46 (t, 1H, Ar–H, J = 8.5 Hz), 7.05 (m, 2H, Ar–H); HRMS: Calcd for $C_{15}H_{11}N_4O_3$, $[M+H]^+$ 295.0831, found 295.0805; Mass m/z: 295.27 $[M+H]^+$.

*2.4.2.3. 2-(4-(Diethylamino)-2-hydroxyphenyl)-7,8-dihydro-3H-imidazo[4,5-f]phthalazine-6,9-dione **(8'a)**.* Yield: 90%; Melting point: 188–190 °C; FT-IR: 3312 (−OH), 2977 (−NH), 1706 (−C═O amide), 1607, 1581 (C═C, C═N ring stretching), 1347, 1261 (C–O stretching) cm^{-1}; ^1H NMR (DMSO-d_6): δ 11.79 [br s, 3H (2H, −NH and 1H, −OH)], 8.29 (s, 1H, −NH), 8.19 (br s, 1H, Ar–H), 8.01 (br s, 1H, Ar–H), 7.81 (br s, 1H, Ar–H), 6.37 (dd, 1H, Ar–H, J = 2.5 Hz and J = 6.5 Hz), 6.23 (s, 1H, Ar–H), 3.34 (q, 4H, $-NCH_2$), 1.14 (t, 6H, $-CH_3$); ^1H NMR (D_2O exchange): δ 8.15 (br s, 1H, Ar–H), 7.02 (d, 1H, Ar–H, J = 7.0 Hz), 7.85 (br s, 1H, Ar–H), 6.38 (d, 1H, Ar–H, J = 8.0 Hz), 6.22 (s, 1H, Ar–H), 3.35 (q, 4H, $-NCH_2$), 1.11 (t, 6H, $-CH_3$); HRMS: Calcd for $C_{19}H_{20}N_5O_3$, $[M+H]^+$ 366.1566, found 366.1534; Mass m/z: 366.19 $[M+H]^+$.

*2.4.2.4. 2-(2-Hydroxyphenyl)-7,8-dihydro-3H-imidazo[4,5-f]phthalazine-6,9-dione **(8'b)**.* Yield: 78%; Melting point: 192–194 °C; FT-IR: 3383 (−OH), 2855 (−NH), 1659 (−C═O amide), 1608, 1589 (C═C, C═N ring stretching), 1348, 1294 (C–O stretching) cm^{-1}; ^1H NMR (DMSO-d_6): δ 12.62 (br s, 1H, −OH), 11.95 (br s, 1H, −NH), 11.71 (br s, 2H, −NH), 8.46 (br s, 1H, Ar–H), 8.17 (br s, 1H, Ar–H), 7.87 (br s, 1H, Ar–H), 7.40 (t, 1H, Ar–H, J = 8.5 Hz), 7.08 (d, 1H, Ar–H, J = 8.0 Hz), 7.03 (t, 1H, Ar–H, J = 8.5 Hz); ^1H NMR (D_2O exchange): δ 8.27 (br s, 1H, Ar–H), 8.15 (d, 1H, Ar–H, J = 8.0 Hz), 7.93 (br s, 1H, Ar–H), 7.41 (t, 1H, Ar–H, J = 7.5 Hz), 7.08 (d, 1H, Ar–H, J = 8.0 Hz), 7.03 (t, 1H, Ar–H, J = 7.5 Hz); HRMS: Calcd for $C_{15}H_{11}N_4O_3$, $[M+H]^+$ 295.0831, found 295.0808; Mass m/z: 295.30 $[M+H]^+$.

*2.4.2.5. 2-(2,4-Dihydroxyphenyl)-7,8-dihydro-3H-imidazo[4,5-f]phthalazine-6,9-dione **(8'c)**.* Yield: 86%; Melting point: 180–182 °C; FT-IR: 3332 (−OH), 2980 (−NH), 1687 (−C═O amide), 1618, 1588 (C═C, C═N ring stretching), 1374, 1252 (C–O stretching) cm^{-1}. ^1H NMR (DMSO-d_6): (−OH and −NH proton is exchange in solvent) δ 8.11 (d, 1H, Ar–H, J = 8.5 Hz), 7.96 (d, 1H, Ar–H, J = 8.5 Hz), 7.81 (d, 1H, Ar–H, J = 8.5 Hz), 6.50 (s, 1H, Ar–H), 6.35 (dd, 1H, Ar–H, J = 1.5 Hz and J = 7.0 Hz); ^1H NMR (D_2O exchange): δ 8.09 (d, 1H, Ar–H, J = 8.5 Hz), 7.97 (d, 1H, Ar–H, J = 8.5 Hz), 7.87 (d, 1H, Ar–H, J = 8.5 Hz), 6.56 (s, 1H, Ar–H), 6.37 (d, 1H, Ar–H, J = 7.5 Hz); HRMS: Calcd for $C_{15}H_{11}N_4O_4$, $[M+H]^+$ 311.0780, found 311.1016; Mass m/z: 310.14 $[M]^+$.

3. Results and discussion:

3.1. Synthetic strategy

In the first step, dimethyl-4-nitrophthalate **1** was synthesized by esterification of 4-nitrophthalic acid. Compound **1** on reduction using H_2/Pd–C (10%) gave the compound **2,** which on further acetylation using acetic anhydride in toluene yielded the intermediate **3**. Nitration of the intermediate of **3** with fuming HNO_3 and H_2SO_4 gave a mixture of **4** and **4'**. The mixture of compounds **4** and **4'** was separated by fractional crystallization in methanol and CCl_4, which on deacetylation in concentrated H_2SO_4 gave the intermediates **5** and **5'.** Nitro groups of compound **5** and **5'** were reduced by using H_2/Pd–C (10%) gave the compound **(6** and **6'),** which on further condensation with *o*-hydroxybenzaldehyde **(a-c)** in absolute ethanol containing a catalytic amount of PCl_3 gave **7a–7b** and **7'a–7'c.** Compounds **7a, 7b** and **7a'–7c'** was further heated under reflux in hydrazine hydrate, triethyl amine in methanol to yield desired D-π-A fluorescent compounds **8a–8b** and **8'a–8'c** respectively.

The structures of the compounds were confirmed by FTIR, ^1H NMR, and mass spectral analysis. The protons corresponding to −OH and −NH are not observed in the ^1H NMR spectrum of **7b** which is due to the exchange of protons with the solvent, but in the next step for **8b** both signals (−OH, −NH) were observed (δ 13.56 and δ 12.52) and similar observation is observed in the case of compounds **7'b** and **8'b.** Compounds **7'c** and **8'c** both the −OH and −NH signal was not observed but all the compounds mass spectra is in good agreement with molecular weight.

3.2. ESIPT phenomenon

The synthesized substituted **HPBIs** (linear and angular) **7a–7b, 7'a–7'c** and **8a–8c, 8'a–8'c** contains an acidic −OH group at the 2-position with respective to the benzimidazole ring. The position of the acidic proton of the −OH group and the benzimidazole ═N–

atom is such that there is an existence of the intramolecular hydrogen bonding in the ground state. On excitation the basicity of =N– moiety of the benzimidazole ring increases and the acidity of the hydroxy proton increases. The excitation of the ground state enol (E-Enol) to the excited enol (E-Enol*) is due to the absorption of photon. This E-Enol* form either undergoes ESIPT to form the excited state keto form (K-Keto*) or emits a radiation and returns to the ground state enol form (E-Enol). The excited state keto form (K-Keto*) emits radiation and comes to the ground state keto form (K-Keto) (Fig. 1). But in the case of the barrierless ESIPT, typically the proton of the hydroxyl or amino group, in the excited state migrates to a basic unit is very fast because the distance between acidic proton and basic unit is less than 2 Å. In this way the same molecule either shows broad single emission or dual emission with a large Stokes shift in solvents of different polarity.

3.3. Rotamers and conformers and their ground state energy

The substituted linear and angular **HPBIs** contain a fused imidazole ring (at 3,4 or 4,5-position of dimethylphthalate) having a free phenyl ring with *o*-hydroxyl group which is participating in the proton transfer at the excited state (ESIPT) [39]. In the ground state (S_0), a linear and angular HPBI derivative can exist in equilibrium with several different conformers arising from tautomerism and rotamerism (Fig. 2). Generally planar *syn* form (denoted E*syn*) features an intramolecular hydrogen bond between the acidic hydroxyl (–OH) group and the basic nitrogen (=N) atom [40]. The E*syn* conformer can undergo proton transfer (PT) to form its keto tautomer (denoted K*syn*). These two conformers undergo rotamerization to form their non planar anti forms (denoted E*anti* and K*anti*, respectively). The E*anti* form has its –OH group rotated to the opposite side, relative to that of the planar form. In a protic solvent, the E*anti* conformer can form hydrogen bonds with solvent molecules, but the probability of proton transfer happens to be very remote. DFT computations indicate that in all the solvents, the E*syn* form is more stable than the K*syn* and E*anti* enol form, which is preferred in the ground state (Tables S1–S7). In the ground state keto forms are prohibitively higher in energy such that they do not exist. The absence of long wavelength absorption in the absorptive species is also indicative of the non-existence of the keto form.

3.4. Photo-physical properties

The photophysical behaviour of the compounds has been examined by measuring absorption and fluorescence spectra in different solvents **(7a–7b, 7'a–7'c** in acetone, dichloromethane, methanol, acetonitrile, *N,N'*-dimethylformamide and compounds **8a–8b, 8'a–8'c** in *N,N'*-dimethylformamide, dimethyl sulphoxide, acetic acid) (Table 1, Table S8–S11).

All of the compounds show a well-resolved absorption profile in the range of 334–410 nm with molar extinction coefficient values (ε) in agreement with π–π^* transitions (Fig. 3, Fig. S1–S10). All the compounds show single absorption in the solvents studied. The theoretical vertical excitation values of the compounds are in good agreement with the experimental absorption; the difference between the theoretical and experimental values is less than 45 nm in all the solvents studied.

The red shifted absorption maxima indicates that the *o*-hydroxy and *N,N*-diethylamino moiety present in the compounds **7a, 7'a, 8a, 8'a** (364 nm, 385 nm, 385 nm, 390 nm) has a stronger electron donating effect than in **7b, 7'b, 8b, 8'b** (343 nm, 349 nm, 342 nm, 356 nm) devoid of the *N,N*-diethylamino group respectively. These results also showed that the compounds **7a, 7'a, 8a, 8'a** exhibited red shifted emission as compared to the compounds **7b, 7'b, 8b, 8'b**. The introduction of electron donor group in the $C_{2'}$, $C_{4'}$ positions induced intramolecular charge transfer and mesomeric dipole moment. When compared with unsubstituted analogues [25] of the molecules **7a, 7'a, 8a, 8'a** and **7b, 7'b, 8b, 8'b** latter have shown a red shifted absorption. The electron withdrawing effect of diester **(7a–7b, 7'a–7'c)** and cyclic amide **(8a–8b, 8'a–8'c)** groups have induced efficient donor to acceptor charge transfer. The molecules **7a, 7'a, 8a, 8'a** and **7b, 7'b, 8b, 8'b** absorbs at longer wavelength in DMF as compared to their unsubstituted analogue which absorb at 229 nm and 246 nm respectively. It is also observed that molecules **7a, 7'a, 8a, 8'a** absorbs at longer wavelength than the nitro substituted (333 nm) analogue. Nitro group being strong electron

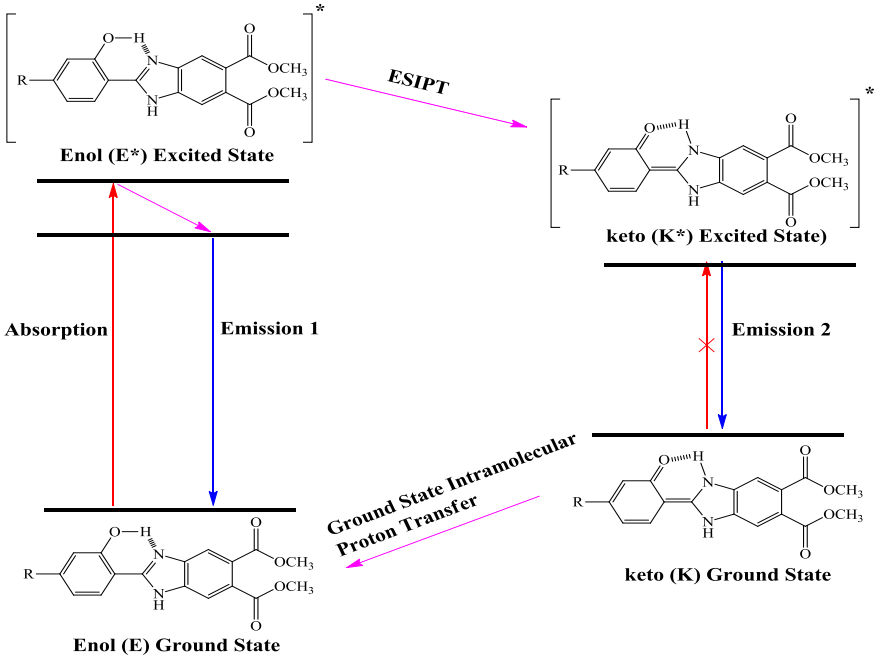

Fig. 1. Excited state intramolecular proton transfer (ESIPT) pathway.

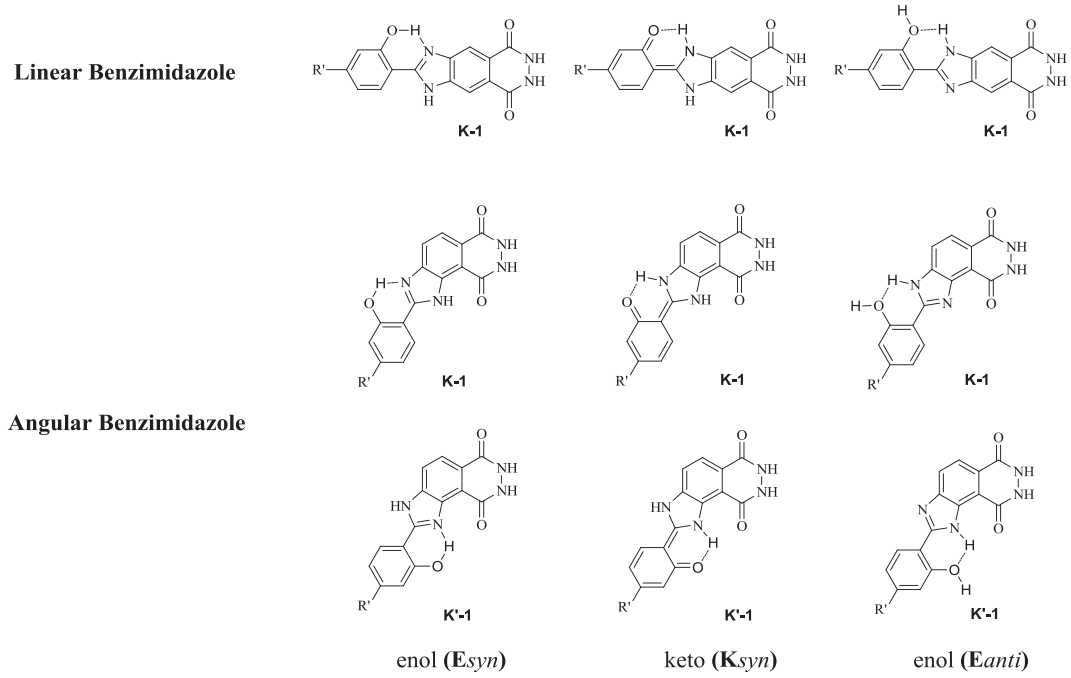

Fig. 2. Possible conformers and tautomers of linear and angular Benzimidazole.

withdrawing group than diester and amide was expected to show a red shift in absorption [25]; however the diester and cyclic amide group affords rigidity and planarity to the molecules and proved to be an efficient electron withdrawer.

The intense absorption of the phthalate and phthalazine **(HPBI)** can be assigned to HOMO–LUMO transition in all solvents. The frontier molecular orbital (FMO) 105, 85, 89, 96, 76, 80 is HOMO and FMO 106, 86, 90, 97, 77, 81 is LUMO in all cases of compounds **7a–7'a, 7b–7'b, 7'c, 8a–8'a, 8b–8'b, 8'c** respectively. It also observed that in phthalate **(7a–7b, 7'a–7'c)** HPBI, –OH, $-N(C_2H_5)_2$ acts as an electron donor; HOMO–LUMO transition is accompanied by the transfer of electrons toward the dimethyl phthalate core. It is observed that in the HOMO the electron density is distributed on the *o*-hydroxyphenyl ring and benzimidazole core. While in the phthalazine **(8a–8b, 8'a–8'c)** HPBI, electron density is concentrated on the phthalazine nitrogen atoms in the HOMO. On excitation of both phthalate and phthalazine to the LUMO, the electron density is redistributed equally throughout the molecules, which all are in one plane (Fig. 4, Fig. S11–S19).

Compound **8'c,** taken as an example, in this case of polar solvent like DMF, HOMO → LUMO (98%) transition is responsible for vertical excitation located at 361 nm with oscillator strength (*f*) 0.731 (Fig. 4), which corresponds to the experimentally observed absorption at 356 nm. A similar trend is observed in all compounds in all other solvents. The solvatochromism study reveals that the absorption wavelength of the compounds **7a, 7b, 7'a, 7'c, 8b, 8'a** are sensitive to solvent polarity. However, the absorption intensity is insensitive to the solvent polarity.

3.5. Emission and solvatofluorism study

The solvatofluorism study reveals that compound **8'c** shows dual emission in DMF and DMSO, while compounds **7a,7b, 7'a, 7'b, 7'c, 8a, 8b, 8'a, 8'b** showed broad single emission in all

Table 1
Observed UV–Visible absorption-emission and computed vertical excitation of the compounds **7a–7b, 7'a–7'c, 8a–8b** and **8'a–8'c** in DMF.

Comp.	Experimental		Stokes shift	Computed (TD-DFT)			%D[e]	Φ
	λ_{max}[a] nm	λ_{max}[b] nm Intensity (au)		Vertical[c] excitation (nm)	*f*[d]	Orbital contribution		
7a	364 (43,670)	507 (9.03)	143	350	0.670	H → L (95%)	3.9	0.08
7b	343 (36,186)	462 (26.42)	123	327	0.652	H → L (97%)	4.7	0.07
7'a	385 (29,378)	515 (10.34)	130	379	0.585	H → L (98%)	1.7	0.06
7'b	349 (24,124)	487 (62.45)	138	355	0.503	H → L (98%)	1.6	0.08
7'c	346 (29,070)	445 (13.19)	99	362	0.644	H → L (98%)	4.5	0.05
8a	385 (66,795)	489 (55.32)	104	360	0.690	H → L (97%)	6.5	0.12
8b	342 (21,756)	439 (28.21)	97	335	0.596	H → L (97%)	2.1	0.15
8'a	390 (53,290)	520 (27.80)	130	387	0.682	H → L (98%)	0.8	0.11
8'b	356 (46,158)	469 (100.8)	116	355	0.551	H → L (98%)	0.3	0.12
8'c	356 (30,380)	405 (24.34)	49	361	0.731	H → L (98%)	1.4	0.13
		515 (20.18)	164					

Φ: Quantum yield in various solvents.
[a] Experimental absorption wavelength.
[b] Experimental emission wavelength.
[c] Computed vertical excitation.
[d] Oscillator strength.
[e] *D*% Deviation between experimental absorption and vertical excitation computed by DFT.

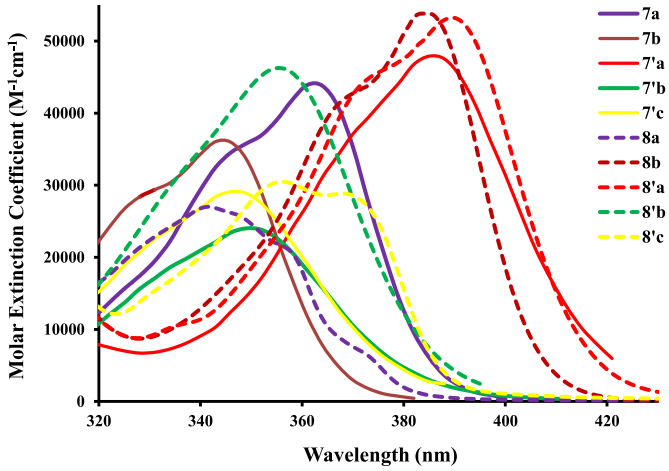

Fig. 3. Absorption spectra of compounds **7a**–**7b, 7'a**–**7'c, 8a**–**8b** and **8'a**–**8'c** in DMF.

Table 2
Observed and the computed emission of the compounds **7a**–**7b, 7'a**–**7'c, 8a**–**8b** and **8'a**–**8'c** in DMF.[a]

Comp.	Experimental emission[b] (nm)		TD-DFT emission[c] (nm)		%D[d]	%D[e]
	Short wavelength	Long wavelength	Short wavelength	Long wavelength		
7a	507	–	433	458	14.6	9.7
7b	462	–	365	449	21.0	2.8
7'a	515	–	521	531	1.2	3.1
7'b	487	–	395	521	18.9	7.0
7'c	445	–	403	511	9.4	14.8
8a	489	–	439	456	10.2	6.7
8b	439	–	362	461	17.5	5.0
8'a	520	–	522	527	0.4	1.3
8'b	469	–	392	520	16.4	10.9
8'c	405	515	399	503	1.5	2.3

[a] Analysis were carried out at room temperature (25 °C).
[b] Observed experiment emission.
[c] Computed using TD-DFT method with the B3LYP/6-31G(d).
[d] % Deviation between experimental short emission and computed enol emission by TD-DFT.
[e] % Deviation between experimental long emission and computed keto emission by TD-DFT.

solvents (Table 2, Table S12–S15, Fig. 5, Fig. S1–S10). It is well-known that the long wavelength emission is attributed to the excited state keto tautomer originating from the excited state enol tautomer in the ESIPT molecules [19]. The driving force behind the proton transfer is the associated intrinsic extra stabilization at the exited state of the keto tautomer. Also, the geometry consideration favours the keto form in the excited state. In compounds **7a,7b, 7'a, 7'b, 7'c, 8a, 8b, 8'a, 8'b** a broad single emission may be due to the barrierless proton transfer because the computed enol and keto emission values are in the range of broad emission obtained experimentally and the distance between –OH proton and benzimidazole nitrogen is less than 2 Å (Fig. S11–S19).

3.6. Relative quantum yield of compounds

The fluorescence quantum yields of the synthesized compounds were determined in different solvents are illustrated in Table 1, Table S8–S11. The fluorescence quantum yields of the compounds are largely dependent on the nature of the substituent and the solvent polarity. Here, decrease in the solvent polarity strongly enhances the fluorescence quantum yields. The compounds **7a**–**7b** and **7'a**–**7'c** showed higher quantum efficiencies in non-polar solvents whereas in polar solvents the quantum yield values were

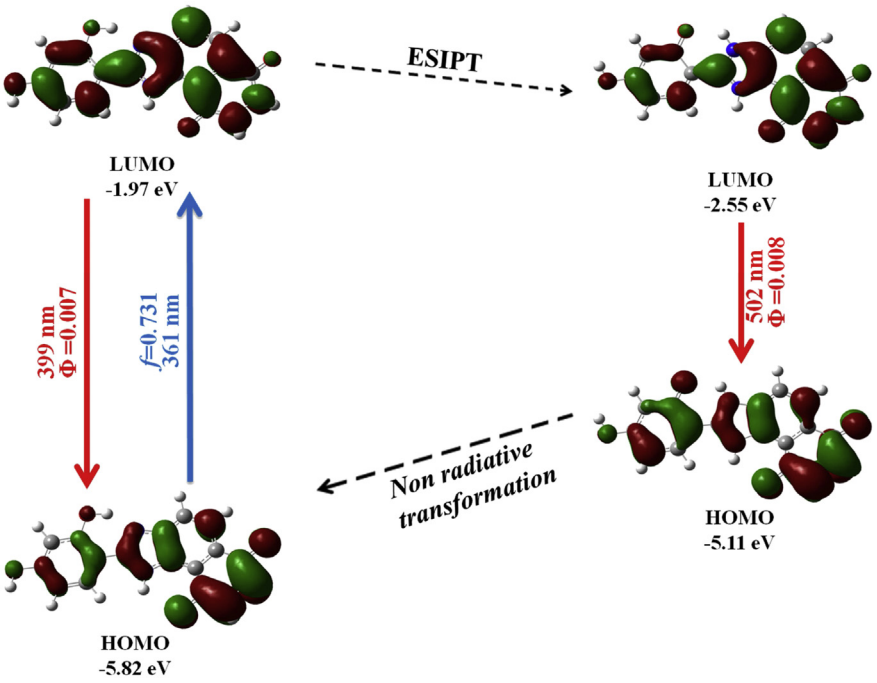

Fig. 4. Representation of the UV–visible absorption and emission of the compound **8'c** in DMF. The vertical excitation related calculations were based on optimized ground state geometry and the emission based calculations were based on optimized excited state geometry at B3LYP/6-31G(d). The HOMO and LUMO energy levels in the excited state are different from those in the ground state. The FMO involved in the vertical excitation (UV–visible absorption: one blue line and emission: two red lines). (For interpretation of the references to colour in this figure legend, the reader is referred to the web version of this article).

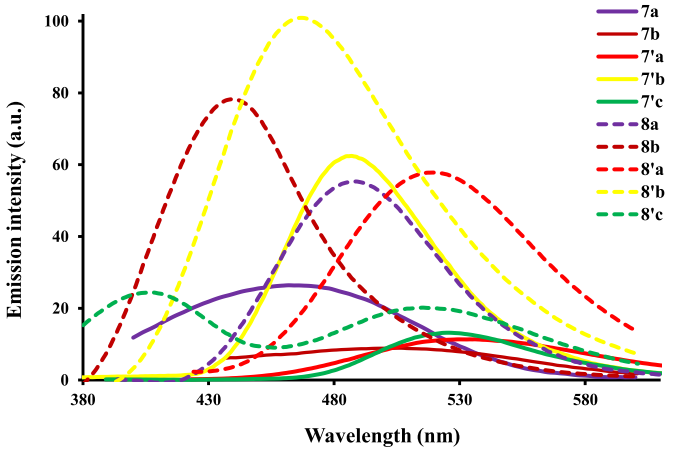

Fig. 5. Emission spectra of compounds **7a–7b, 7'a–7'c, 8a–8b** and **8'a–8'c** in DMF.

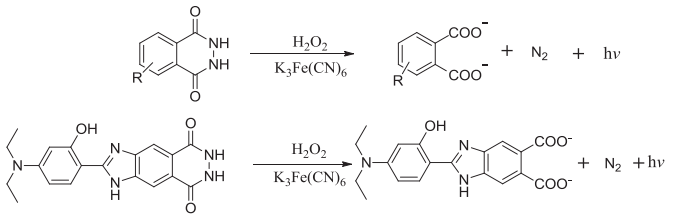

Fig. 6. Chemiluminescence reactions of isoluminol-related compound **(8a)**.

invariably found to be low. The quantum yields of the compounds **8a–8b** and **8'a–8'c** are recorded only in polar solvent due to their solubility. The compounds **7a–7b** and **7'a–7'c** showed the highest quantum yield in DCM. The decreasing order is **7'b** (0.15) > **7a** (0.14) = **7b** (0.14) > **7'a** (0.07) = **7'c** (0.07). The quantum yield values were the lowest in acetonitrile in the increasing order: **7'c** (0.04) < **7'a** (0.05) < **7b** (0.06) = **7'b** (0.06) < **7a** (0.07). While for the compounds **8a–8b** and **8'a–8'c** the quantum yield is higher in DMF the decreasing order is **8b** (0.15) > **8'c** (0.13) > **8a** (0.12) = **8'b** (0.12) > **8'a** (0.11) and lowest in acetic acid increasing order: **8a** (0.04) = **8'b** (0.04) = **8'c** (0.04) < 8b (0.07) = **8'a** (0.07). The compounds **7a–7b, 7'a–7'c** in acetonitrile, DMF and **8a–8b, 8'a–8'c** in acetic acid showed very less emission intensity. The positive solvatokinetic behaviour suggests that a highly polar excited-state population charge transfer state and a non-radiative decay was prominent in these compounds [35].

3.7. Chemiluminescence study

The distinct chemiluminescence properties of isoluminol–luminol type of compounds **8a–8b** and **8'a–8'c** were examined in order to evaluate their use as highly chemiluminescent probes. These compounds **8a–8b** and **8'a–8'c** produce chemiluminescence by reaction with hydrogen peroxide in the presence of potassium hexacyanoferrate(III) in alkaline medium (Fig. 6). The oxidizing reagent concentrations have a major influence on the chemiluminescence intensity (Fig. 7); 2.5–5 mM hydrogen peroxide, 2.5–5 mM potassium hexacyanoferrate(III) and 0.5–2.0 M sodium hydroxide give the highest chemiluminescence intensity. After the addition of the oxidising agents, the chemiluminescence intensity quickly reached a maximum in a few seconds and then almost disappeared within one minute.

Under these optimum reaction conditions, the chemiluminescence intensities of the compounds were determined and summarised in Table 3. In the compounds **8a–8b** and **8'a–8'c** chemiluminescence generation were found approximately 3.5–7.3 times higher than that of isoluminol, and the intensities corresponded to 0.8–1.8 times of the value obtained with luminol itself. The time dependence of the chemiluminescence reaction of the compounds **8a–8b** and **8'a–8'c** and luminol–isoluminol is illustrated in Fig. 8. The chemiluminescence generation is initiated by the addition of the alkaline solution of hydrogen peroxide and potassium hexacyanoferrate(III) to the stock solution. After the addition of the oxidizing reagents the chemiluminescence intensity reached their maxima within 1.5 s, and then decreased rapidly. The chemically excited 3-aminophthalate and 4-aminophthalate ion produced during the oxidizing reaction has been shown to be the light emitter in the chemiluminescence of the luminol **(8'a–8'c)** and isoluminol **(8a–8b).** Therefore, in the newly synthesized luminol–isoluminol type chemiluminophores, the expected light emitting species could be the corresponding dicarboxylate ions (Fig. 6). The fluorescent properties like excitation and emission maxima of the fluorescence and its relative intensities of the species, on the completion of the chemiluminescence reaction are measured, and compared with the conventional luminol–isoluminol analogues (Table 3). The fluorescence intensities of the compounds **8a–8b** and **8'a–8'c** dicarboxylate ions were 4.11–10.80 and 4.6–12.09 times larger than that of 4-aminophthalate anion of the isoluminol and 3-aminophthalate anion of the luminol respectively. These results proposed that the efficiency of the chemiluminescence intensity of the isoluminol–luminol type chemiluminophores is mostly dependent on the fluorescence intensities of the light-emitting species produced during the chemiluminescence reaction. Otherwise, the

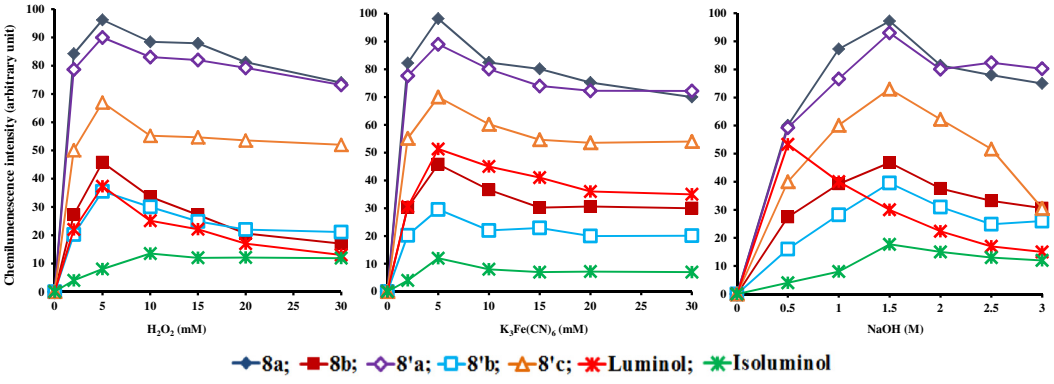

Fig. 7. Effects of concentrations of hydrogen peroxide, potassium hexacyanoferrate(III) and sodium hydroxide on integrated chemiluminescence intensities of compounds Luminol, Isoluminol, **8a–8b** and **8'a–8'c** (a run time of 60 s).

Table 3
Fluorescence excitation and emission maxima and relative intensities (R.F.I.) and Relative chemiluminescence intensities (RCI) of the dicarboxylate anions corresponded to the chemiluminophores.

Chemiluminophore	Excitation (nm)	Emission (nm)	R.F.I.[a]	R.C.I.[b]
8a	389	503	1136	183
8b	394	486	432	89
8'a	385	511	1209	176
8'b	363	501	467	80
8'c	375	498	576	139
Isoluminol	274	470	105	24
Luminol	316	425	100[a]	100[b]

[a] Integrated chemiluminescence intensity of luminol in DMF was taken as 100.
[b] Integrated fluorescence intensity of luminol in DMF was taken as 100.

chemiluminescence spectra of isoluminol and luminol type compounds and the fluorescence emission spectra of the corresponding phthalate ion are almost identical [41,42]. Thus, compounds **8a**–**8b** and **8'a, 8'c** were expected to generate chemiluminescence at longer wavelength as compared to the isoluminol and luminol respectively, which means that the use of these compounds as the chemiluminescence labelling reagents might be profitable.

3.8. *Structural properties of compounds **7a**–**7b**, **7'a**–**7'c**, **8a**–**8b** and **8'a**–**8'c***

In the ESIPT process the proton is transferred in the excited state, after excitation of the enol form to first excited state singlet undergoes redistribution of electron densities leading to a different geometry favouring a proton transfer and ultimately forms the excited state keto, which becomes an emissive species fluorescing a longer wavelength. In the excited state, the hydrogen attached to oxygen approaches to the basic nitrogen of the imidazole unit via a six-membered hydrogen bonding framework for the transfer of proton. Planarity of the molecule is also a major factor for the proton transfer in the excited state enol. This ESIPT phenomenon is explained by using the TD-DFT computation. Changes in bond lengths, bond angles, Mulliken charges of the ground and excited state of the optimized geometries of the enol as well as keto forms are explained with the help of TD-DFT.

As a representative example of the dicarboxylate **HPBI**, the structural view of compound **7a** in the ground and the excited state of the enol as well as the keto form are presented in Fig. 9 and the structures of compounds **7b**, **7'a**–**7'c, 8a**–**8b** and **8'a**–**8'c** are summarized in (Table S16–S23). In the case of compound **7a** in methanol, the hydrogen bonding distance between the N_{28}–H_{30} decreases by 0.037 Å from the ground state enol (1.728 Å) to the excited state enol (1.691 Å), The bond distances between O_{29}–H_{30}

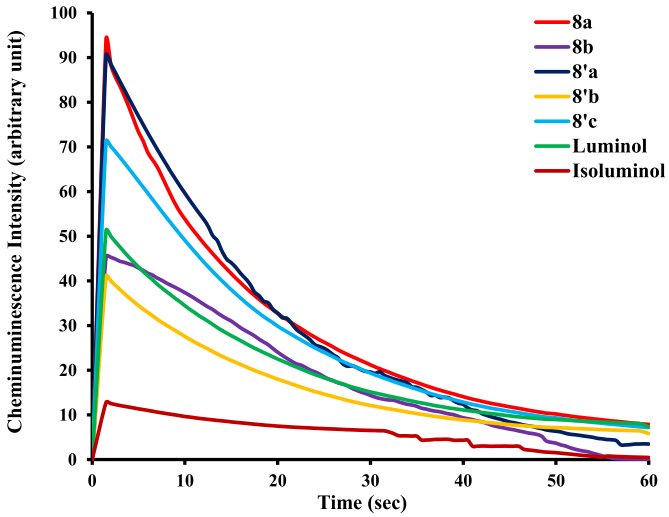

Fig. 8. Time dependence of the chemiluminescence reaction of the Isoluminol, luminol and its analogue **(8a–8b)** and **(8'a–8'c)**.

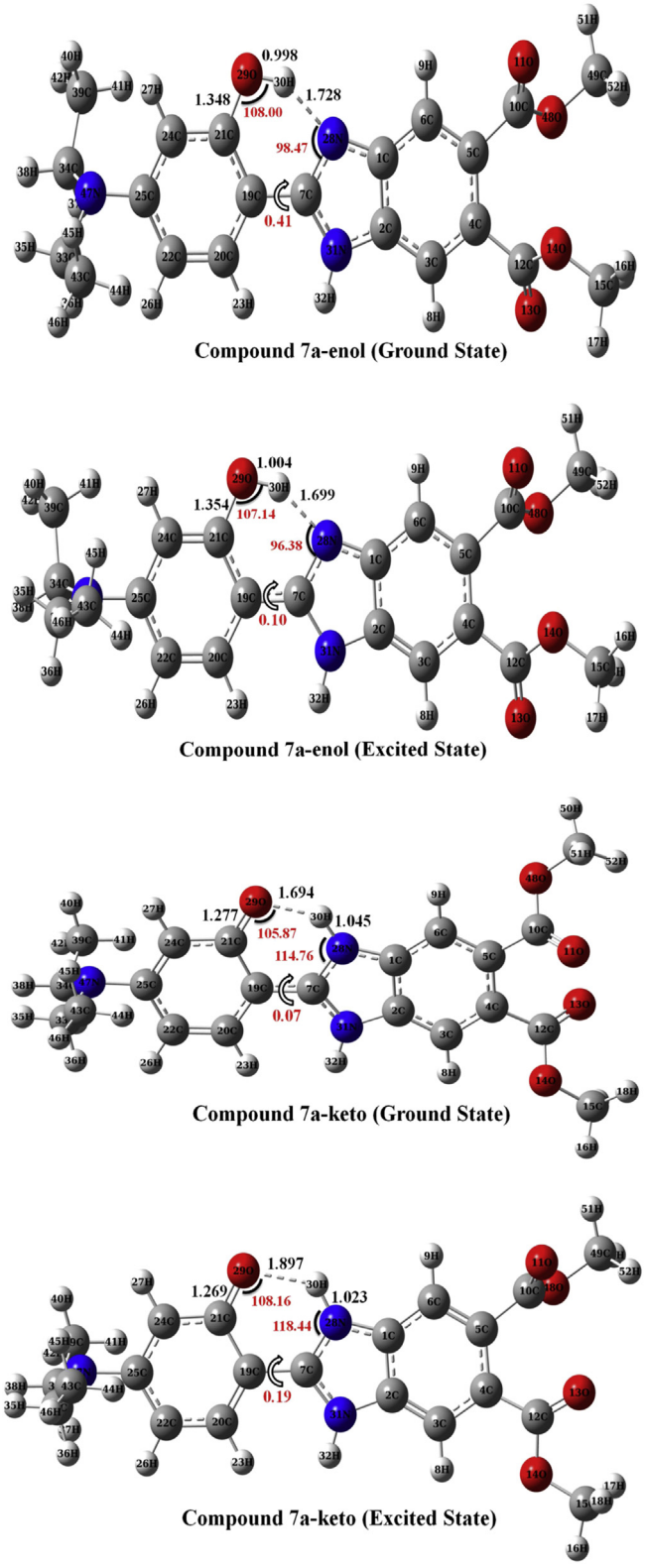

Fig. 9. Structural view of compound **7a** in ground and excited state of enol as well as keto form.

Table 4
Dipole moment (μ in Debye) of compounds **7a**–**7b**, **7'a**–**7'c**, **8a**–**8b** and **8'a**–**8'c**.

Compounds	[a]Enol μ_g	[b]Enol μ_e	[b]Enol μ_e / [a]Enol μ_g	[a]Keto μ_g	[b]Keto μ_e	[b]Keto μ_e / [a]Keto μ_g	[c]Experimental Dipole moment	%D
7a	4.16	4.02	0.97	6.15	8.97	1.46	1.83	47
7b	4.35	4.79	1.10	3.76	3.92	1.04	0.41	63
7'a	5.76	6.54	1.14	5.40	4.87	0.90	0.02	98
7'b	4.90	4.57	0.93	4.95	4.56	0.92	3.17	71
7'c	6.32	6.89	1.09	4.43	4.35	0.98	0.33	70
8a	4.58	4.95	1.08	4.88	5.02	1.03	1.5	28
8b	3.80	3.56	0.94	4.47	4.12	0.92	0.25	73
8'a	3.22	5.67	1.76	3.71	3.87	1.04	5.6	69
8'b	3.40	3.03	0.89	4.64	4.43	0.95	0.7	22
8'c	4.86	4.58	0.94	3.34	3.02	0.90	0.8[d]	15[f]
							1.03[e]	9[g]

[a] Dipole moment of compound in ground state.
[b] Dipole moment of compound in excited state.
[c] Experimental dipole moment obtained from solvatochromism data using Bakhshiev and Kawski–Chamma–Viallet correlations.
[d] Dipole moment at short wavelength emission obtained from solvatochromism data using Bakhshiev and Kawski–Chamma–Viallet correlations.
[e] Dipole moment at long wavelength emission obtained from solvatochromism data using Bakhshiev and Kawski–Chamma–Viallet correlations.
[f] (%*D*) % Deviation between experimental and computed dipole moment for short wavelength emission.
[g] (%*D*) % Deviation between experimental and computed dipole moment for long wavelength emission.

increase by 0.006 Å from the ground state enol (0.998 Å) to the excited enol (1.004 Å). While the charges on N_{28}, O_{29} and H_{30} were increased by 0.005|e|, 0.001|e| and 0.002|e| from the ground state enol to the excited state enol respectively. The charges on N_{28} increase more than O_{29} in the excited state enol which means that the acidic proton (H_{30}) approaches near to the basic nitrogen (N_{28}) via hydrogen bonding. The bond distance between O_{29}–C_{21} and N_{28}–C_7 increases by 0.006 Å and 0.030 Å from the ground state enol (1.349 Å and 1.333 Å) to the excited state enol (1.356 Å and 1.364 Å) which is decreased by 0.086 Å and 0.020 Å in the case of excited keto form (1.269 Å and 1.343 Å) respectively. In addition to this, the bond angle H_{30}–O_{29}–C_{21} and H_{30}–N_{28}–C_7 is decreases by 0.59° and 1.70° from the ground state enol (108.01° and 98.47°) to the excited state enol (107.42° and 96.77°) respectively. In this pathway, proton (H_{30}) approaches the nitrogen (N_{28}) of imidazole unit in the excited state enol form. The H_{30} transfer to N_{28} leads to formation excited state keto form with N_{28}–H_{30} and O_{29}–H_{30} bond distance are 1.023 Å and 1.897 Å, which further returns to the ground state keto conformer with bonding distance are 1.044 Å and 1.703 Å respectively. The above observations indicate that the proton (H_{30}) approaches to oxygen (O_{29}), the hydrogen bonding distance in excited state keto form decreases by 0.194 Å from 1.897 to 1.703 Å and it is immediately converted to the ground state keto form then to the ground state enol form. Similar structural behaviour is observed for the compounds **7b**, **7'a**–**7'c, 8a**–**8b** and **8'a**–**8'c.**

3.9. Effect of solvent polarity on the ground and excited state dipole moments

The fluorescence properties and dipole moment are affected by the solvent polarity because of their interaction with solute or hydrogen bonding with heteroatom present in the solute. Geometry of the compound at the ground and the excited state decide their electronic behaviour. The effect of the solvent polarity on the photophysical properties clearly indicates that in the excited state the dipolar characteristics of compounds change, which means that solvatochromic data gives an efficient tool to understand the change in dipole moment in the first excited state.

Here, we report the ground and excited state dipole moments of the compounds **7a**–**7b, 7'a**–**7'c, 8a**–**8b** and **8'a**–**8'c** by using Bakhshiev [43] and Kawski–Chamma–Viallet correlations [44,45]. This method is based on a linear relation between the absorption, emission maxima and solvent polarity functions (E_T^N) [46–48] which depend both on the relative permittivity (ε) and refractive index (η) of the solvent. The polarity function of solvent has been taken from the literature [49].

The dipole moment ratio of the excited state to the ground state of the compounds **7a**–**7b, 7'a**–**7'c, 8a**–**8b** and **8'a**–**8'c** were calculated by using the solvatochromic data and polarity function of the solvents. The experimental dipole moment values were compared with the computed dipole moments in the vacuum phase by DFT and TD-DFT are summarized in Table 4. The dipole moment obtained from long wavelength emission data compared with ratio of dipole moment of excited state keto and ground state keto form in vacuum phase. These results clearly signify that a large difference was observed between the dipole moment obtained from solvatochromism data and the computed dipole moment.

4. Conclusion

In this paper we have reported new chemiluminescent analogues containing an inbuilt ESIPT residue and their photophysical and chemiluminescence properties by reaction with hydrogen peroxide in the presence of potassium hexacyanoferrate (III) in an alkaline medium. Compounds **8a, 8b, 8'a, 8'b** and **8'c** can be used promising candidate for chemiluminescent probes. Photophysical properties of the compounds were supported by DFT and it was observed that the computational results are in good agreement with the theoretical observations. All the compounds except **8'c** show a single broad emission peak in polar as well as in non-polar solvents. The barrierless proton transfer is proved by DFT; computed enol and keto emission values are in the range of broad emission obtained experimentally and the distance between acidic proton and basic nitrogen is less than 2 Å.

Acknowledgements

The authors are greatly thankful to TIFR, SAIF-I.I.T. Mumbai for recording the ^{1}H NMR, ^{13}C NMR and Mass spectra. One of the authors Mininath S. Deshmukh is grateful to CSIR, New Delhi for the award of a research fellowship.

Appendix A. Supplementary data

Supplementary data related to this article can be found at http://dx.doi.org/10.1016/j.dyepig.2014.08.009.

References

[1] Todoroki K, Ohba Y, Zaitsu K. Chemiluminescence characteristics of N-(4-substituted Benzyl)isoluminol. Chem Pharm Bull (Tokyo) 2000;48:2011–3.
[2] Yoshida H, Ureshino K, Ishida J, Nohta H, Yamaguchi M. Chemiluminescent properties of some luminol related compounds (II). Dye Pigment 1999;41:177–82.
[3] Spurlin SR, Cooper MM. A ChemiluminesClent precolumn labelling reagent for high-performance liquid chromatography of amino acids. Anal Lett 1986;19:2277–83.
[4] Kawasaki T, Maeda M, Tsuji A. Chemiluminescence high-performance liquid chromatography using N-(4-aminobutyl)-N-ethylisoluminol as a precolumn labelling reagent. J Chromatogr A 1985;328:121–6.
[5] Steijger OM, Lingeman H, Brinkman UAT, Holthuis JJM, Smilde AK, Doornbos DA. Liquid chromatographic analysis of carboxylic acids using N-(4-aminobutyl)-N-ethylisoluminol as chemiluminescent label: determination of ibuprofen in saliva. J Chromatogr B Biomed Sci Appl 1993;615:97–110.
[6] Ishida J, Yamaguchi M, Nakahara T, Nakamura M. 4,5-Diaminophthalhy drazide as a highly sensitive chemiluminescence reagent for α-keto acids in liquid chromatography. Anal Chim Acta 1990;231:1–6.
[7] Ishida J, Yakabe T, Nohta H, Yamaguchi M. 6-Aminomethylphthalhydrazide as a highly sensitive chemiluminescence derivatization reagent for 5-hydroxyindoles in liquid chromatography. Anal Chim Acta 1997;346:175–81.
[8] Gundermann K-D, Drawert M. Konstitution und Chemilumineszenz, I. Sterische Resonanzhinderung bei alkylierten Amino-phthalhydraziden. Chem Ber 1962;95:2018–26.
[9] Gundermann K-D, Horstmann W, Bergmann G. Konstitution und Chemilumineszenz, II. Synthese und Chemilumineszenz-Verhalten von 7-Dialkylamino-naphthalin-dicarbonsäure-(1.2)-hydraziden. Justus Liebigs Ann Chem 1965;684:127–41.
[10] Wu J, Liu W, Ge J, Zhang H, Wang P. New sensing mechanisms for design of fluorescent chemosensors emerging in recent years. Chem Soc Rev 2011;40:3483–95.
[11] Kwon JE, Park SY. Advanced organic optoelectronic materials: harnessing excited-state intramolecular proton transfer (ESIPT) process. Adv Mater 2011;23:3615–42.
[12] Park S, Kwon JE, Kim SH, Seo J, Chung K, Park S-Y, et al. A White-Light-Emitting molecule: frustrated energy transfer between constituent emitting centers. J Am Chem Soc 2009;131:14043–9.
[13] Taki M, Wolford JL, O'Halloran TV. Emission ratiometric imaging of intracellular zinc: design of a benzoxazole fluorescent sensor and its application in two-photon microscopy. J Am Chem Soc 2003;126:712–3.
[14] Ohshima A, Momotake A, Arai T. A new fluorescent metal sensor with two binding moieties. Tetrahedron Lett 2004;45:9377–81.
[15] Rodembusch FS, Brand FR, Corrêa DS, Pocos JC, Martinelli M, Stefani V. Transition metal complexes from 2-(2′-hydroxyphenyl)benzoxazole: a spectroscopic and thermogravimetric stability study. Mater Chem Phys 2005;92:389–93.
[16] Ríos Vázquez S, Ríos Rodríguez MC, Mosquera M, Rodríguez-Prieto F. Excited-state intramolecular proton Transfer in 2-(3′-Hydroxy-2′-pyridyl)benzoxazole. Evidence of coupled proton and charge transfer in the excited state of some o-Hydroxyarylbenzazoles. J Phys Chem A 2007;111:1814–26.
[17] Luxami V, Kumar S. Molecular half-subtractor based on 3,3[prime or minute]-bis(1H-benzimidazolyl-2-yl)[1,1[prime or minute]]binaphthalenyl-2,2[prime or minute]-diol. New J Chem 2008;32:2074–9.
[18] Fahrni CJ, Henary MM, VanDerveer DG. Excited-state intramolecular proton Transfer in 2-(2′-Tosylaminophenyl)benzimidazole. J Phys Chem A 2002;106:7655–63.
[19] Zhao J, Ji S, Chen Y, Guo H, Yang P. Excited state intramolecular proton transfer (ESIPT): from principal photophysics to the development of new chromophores and applications in fluorescent molecular probes and luminescent materials. Phys Chem Chem Phys 2012;14:8803–17.
[20] Frey W, Elsaesser T. Femtosecond intramolecular proton transfer of vibrationally hot molecules in the electronic ground state. Chem Phys Lett 1992;189:565–70.
[21] Schwartz BJ, Peteanu LA, Harris CB. Direct observation of fast proton transfer: femtosecond photophysics of 3-hydroxyflavone. J Phys Chem 1992;96:3591–8.
[22] Henary MM, Wu, Cody J, Sumalekshmy S, Li J, Mandal S, et al. Excited-state intramolecular proton Transfer in 2-(2′-Arylsulfonamidophenyl)benzimidazole Derivatives: the effect of donor and acceptor substituents. J Org Chem 2007;72:4784–97.
[23] Phatangare KR, Gupta VD, Tathe AB, Padalkar VS, Patil VS, Ramasami P, et al. ESIPT inspired fluorescent 2-(4-benzo[d]oxazol-2-yl)naphtho[1,2-d]oxazol-2-yl)phenol: experimental and DFT based approach to photophysical properties. Tetrahedron 2013;69:1767–77.
[24] Patil VS, Padalkar VS, Phatangare KR, Gupta VD, Umape PG, Sekar N. Synthesis of new ESIPT-fluorescein: photophysics of pH sensitivity and fluorescence. J Phys Chem A 2011;116:536–45.
[25] Padalkar V, Tathe A, Gupta V, Patil V, Phatangare K, Sekar N. Synthesis and photo-physical characteristics of ESIPT inspired 2-Substituted benzimidazole, benzoxazole and benzothiazole fluorescent derivatives. J Fluoresc 2012;22:311–22.
[26] Brouwer AM. Standards for photoluminescence quantum yield measurements in solution (IUPAC technical report). Pure Appl Chem 2011;83:2213–28.
[27] Frisch MJ, Trucks GW, Schlegel HB, Scuseria GE, Robb MA, Cheeseman JR, et al. Gaussian 09 C.01; 2009.
[28] Treutler O, Ahlrichs R. Efficient molecular numerical integration schemes. J Chem Phys 1995;102:346.
[29] Becke A. A new mixing of Hartree-Fock and local density functional theories. J Chem Phys 1993;98:1372.
[30] Lee C, Yang W, Parr RG. Development of the Colle-Salvetti correlation-energy formula into a functional of the electron density. Phys Rev B 1988;37:785–9.
[31] Li H, Niu L, Xu X, Zhang S, Gao F. A comprehensive therotical investigation of intramolecular proton transfer in the excited states for some newly-designed diphenylethylene derivatives bearing 2-(2-Hydroxy-Phenyl)-Benzotriazole Part. J Fluoresc 2011;21:1721–8.
[32] Bauernschmitt R, Ahlrichs R. Treatment of electronic excitations within the adiabatic approximation of time dependent density functional theory. Chem Phys Lett 1996;256:454–64.
[33] Furche F, Rappoport D. Density functional theory for excited states: equilibrium structure and electronic spectra. In: Olivucci M, editor. Computational Photochemistry. Amsterdam: Elsevier; 2005. p. 93.
[34] Wiberg KB. Ab initio molecular orbital theory by W. J. Hehre, L. Radom, P. v. R. Schleyer, and J. A. Pople, John Wiley, New York, 548pp. Price: 79.95 (1986). J Comput Chem 1986;7:379.
[35] Lakowicz JR. Principles of fluorescence spectroscopy. 2nd ed. New York: Kluwer Academic; 1999.
[36] Valeur B. Molecular fluorescence: principles and applications. Weinheim: Wiley-VCH Verlag GmbH; 2001.
[37] Cossi M, Barone V, Cammi R, Tomasi J. Ab initio study of solvated molecules: a new implementation of the polarizable continuum model. Chem Phys Lett 1996;255:327–35.
[38] Williams RL, Shalaby SW. Heterocyclic studies: new heterocyclic ring systems from isomeric dimethyl diaminophthalates. J Heterocycl Chem 1973;10:891–8.
[39] Magde D, Wong R, Seybold PG. Fluorescence quantum yields and their relation to lifetimes of rhodamine 6G and fluorescein in nine solvents: improved absolute standards for quantum yields. Photochem Photobiol 2002;75:327–34.
[40] Tsai H-HG, Sun H-LS, Tan C-J. TD-DFT study of the excited-state potential energy surfaces of 2-(2′-Hydroxyphenyl)benzimidazole and its amino derivatives. J Phys Chem A 2010;114:4065–79.
[41] Yoshida H, Nakao R, Nohta H, Yamaguchi M. Chemiluminescent properties of some luminol-related compounds — Part 3. Dye Pigment 2000;47:239–45.
[42] Ishida J, Takada M, Yakabe T, Yamaguchi M. Chemiluminescent properties of some luminol related compounds. Dye Pigment 1995;27:1–7.
[43] Bakhshiev N. Universal intermolecular interactions and their effect on the position of the electronic spectra of molecules in two-component solutions. Opt Spectrosc 1962;13:24.
[44] Kawski A. Dipolmomente einiger Naphthole im Grund- und Anregungszustand. Naturwissenschaften 1964;51:82–3.
[45] Chamma A, Viallet PC. Determination du moment dipolaire d'une molecule dans un etat excite singulet. Acad Sci Paris Ser C 1970;270:1901–4.
[46] Biradar DS, Siddlingeshwar B, Hanagodimath SM. Estimation of ground and excited state dipole moments of some laser dyes. J Mol Struct 2008;875:108–12.
[47] Nowak K, Wysocki S. An experimental and theoretical study of dipole moments of N-[4-(9-acridinylamino)-3-methoxyphenyl]methanesulfonamide. Spectrochim Acta Part A Mol Biomol Spectrosc 2008;70:805–10.
[48] Sharma N, Jain SK, Rastogi RC. Solvatochromic study of excited state dipole moments of some biologically active indoles and tryptamines. Spectrochim Acta Part A Mol Biomol Spectrosc 2007;66:171–6.
[49] Reichardt C. Solvents and related titles from WILEY-VCH organic synthesis workbook II chemical synthesis using supercritical fluids. Upd. 3rd ed. WILEY-VCH Verlag; 2003.